Journal of Pharmaceutical and Biomedical Analysis 95 (2014) 68–75

Contents lists available at ScienceDirect

Journal of Pharmaceutical and Biomedical Analysis

journal homepage: www.elsevier.com/locate/jpba

Short communication

Characterization of rational biomarkers accompanying fever in yeast-induced pyrexia rats using urine metabolic footprint analysis

Mingxing Guo[a,1], Hao Gu[b,1], Yuelin Song[c], Long Peng[a], Haiyu Liu[a], Li Zhang[a], Zhaozhou Lin[b], Yun Wang[b,*], Xiaoyan Gao[a,**], Yanjiang Qiao[b]

[a] Science Experiment Center for Traditional Chinese Medicine, Beijing University of Chinese Medicine, No. 11, North Third Ring Road, Chaoyang District, Beijing 100029, PR China
[b] Key Laboratory of TCM-Information Engineering of State Administration of Traditional Chinese Medicine, School of Chinese Materia Medica, Beijing University of Chinese Medicine, South of Wangjing Middle Ring Road, Chaoyang District, Beijing 100102, PR China
[c] Modern Research Center for Traditional Chinese Medicine, Beijing University of Chinese Medicine, No. 11, North Third Ring Road, Chaoyang District, Beijing 100029, PR China

ARTICLE INFO

Article history:
Received 2 September 2013
Received in revised form 13 February 2014
Accepted 15 February 2014
Available online 26 February 2014

Keywords:
Metabolic footprint analysis
Biomarkers
Yeast-induced pyrexia
Ultra performance liquid chromatography
Quadrupole time-of-flight mass spectrometry

ABSTRACT

Fever is a prominent feature of diseases and is an ongoing process that is always accompanied by metabolic changes in the body system. Despite the success of temperature regulation theory, the underlying biological process remains unclear. To truly understand the nature of the febrile response, it is crucial to confirm the biomarkers during the entire biological process. In the current study, a 73-h metabolic footprint analysis of the urine from yeast-induced pyrexia rats was performed using ultra-performance liquid chromatography coupled with quadrupole time-of-flight mass spectrometry. Potential biomarkers were selected using orthogonal partial least squares-discriminate analysis (OPLS-DA), the rational biomarkers were verified by Pearson correlation analysis, and the predictive power was evaluated using receiver operator characteristic (ROC) curves. A metabolic network constructed using traditional Chinese medicine (TCM) grammar systems was used to validate the rationality of the verified biomarkers. Finally, five biomarkers, including indoleacrylic acid, 3-methyluridine, tryptophan, nicotinuric acid and PI (37:3), were confirmed as rational biomarkers because their correlation coefficients were all greater than 0.87 and because all of the correlation coefficients between any pair of these biomarkers were higher than 0.75. The areas under the ROC curves were all greater than 0.84, and their combined predictive power was considered reliable because the greatest area under the ROC curve was 0.968. A metabolic network also demonstrated the rationality of these five biomarkers. Therefore, these five metabolites can be adopted as rational biomarkers to reflect the process of the febrile response in inflammation-induced pyrexia.

1. Introduction

Fever is one of the main acute-phase reaction symptoms in a variety of diseases, particularly in infectious diseases, inflammatory diseases and in autoimmune diseases [1,2]. Although there are two thermoregulatory circuitries that have been reported, *i.e.*, the humoral pathway and the neural pathway [3], numerous endogenous substances participating in the febrile response and their dynamic changing process have not been clarified. Screening rational biomarkers from numerous metabolites that are directly correlated with body temperature and exploring the network relation between biomarkers and febrile response-related inflammatory mediators and/or cytokines that play determinant roles is important for understanding the mechanism of pyrexia.

At present, several pyrexia-related animal models have been established and validated to explore the pathogenesis and pathophysiology of pyrexia [4–6]. Among these models, yeast-induced pyrexia has been widely utilized to study the development of the pyretic bodies induced by inflammation [7–9]. Yeast-induced

* Corresponding author at: Key Laboratory of TCM-Information Engineering of State Administration of Traditional Chinese Medicine, School of Chinese Materia Medica, Beijing University of Chinese Medicine, Beijing, PR China.
Tel.: +86 1084738620; fax: +86 1084738620.
** Corresponding author at: Science Experiment Center for Traditional Chinese Medicine, Beijing University of Chinese Medicine, Beijing, PR China.
Tel.: +86 010 64286401; fax: +86 010 64286052.
E-mail addresses: wangyun@bucm.edu.cn (Y. Wang), gaoxiaoyan0913@sina.com (X. Gao).
[1] Co-first authors: Mingxing Guo and Hao Gu.

http://dx.doi.org/10.1016/j.jpba.2014.02.011
0731-7085/

pyrexia has been reported as a pathogenic fever that leads to an intense inflammatory reaction caused by ulceration at the injection site [10]. Until now, the mechanism of the yeast-induced pyrexia model has not been completely clarified, in spite of its wide adoption.

In our previous study, we have proven that the yeast-induced febrile response is a dynamic pathological developing process, during which the changing trend of metabolic profile clustering was consistent with the changing trend of the rectal temperature in yeast-induced pyrexia rats, and impaired tryptophan metabolism was demonstrated to be related to the fever [11]. With subsequent research, we found that the selection of time-points was important for utilizing metabolomic tools to reveal the underlying biological processes of acute metabolic diseases, such as fever [12]. If only one single time-point instead of for the continuous changing process was adopted, a cross-sectional for the study object would occur. Therefore, based on our previous study, we perform a dynamic study to reveal for the first time the dynamic changing process of organisms.

In metabolomic research, the course from potential biomarkers to clinical indicators or terminal indexes is complex and time-consuming. Metabolites identified from an early stage of metabolomics should undergo larger, prospective, externally validations in clinical cohorts before their future employment as practical biomarkers [13], thus demanding numerous studies [14]. Among the many published metabolomic studies that focus on biomarker discovery, few researchers have reported to the process by which the selected range of potential biomarkers is narrowed. Due to the complexity of the fever mechanism, it is difficult to elucidate the exact metabolism of potential biomarkers. Fortunately, the available Pearson correlation analysis, receiver operator characteristic (ROC) curves and traditional Chinese medicine (TCM) grammar systems provide good selecting and verifying features. Pearson correlation analysis can be used to assess the relation between potential biomarkers and clinical indicators. ROC curve analysis is widely considered to be the most objective and statistically valid method for biomarker performance evaluation [15]. Moreover, TCM grammar systems, which provide formal tools to study the entangled hierarchies in biological systems and to control the generation of emergence in certain conditions by entity grammar systems [16], can integrate the concerned pieces of parsed knowledge to better elucidate the relations between biomarkers and pyrexia. In this paper, we investigated for the first time the relations between potential biomarkers at different time-points using a metabolic footprint and a pharmacological index, aiming to discover more rational biomarkers of the febrile response in yeast-induced pyrexia rats. In addition, the filtered biomarkers were validated using ROC curve analysis and a network constructed using TCM grammar systems. This network was composed of proven inflammatory mediators and cytokines relating to the febrile response. The results obtained in current study are expected to provide a practical strategy to identify biomarkers for studying the mechanism of inflammation-induced pyrexia and other acute metabolic diseases.

2. Materials and methods

2.1. Chemicals and reagents

Yeast was purchased from Mauri Food Co. Ltd. (Hebei, China). HPLC grade methanol and acetonitrile were acquired from Baker Company (Baker Inc., USA). Ultra high purity water was prepared by Millipore-Q SAS 67120MOLSHEIM (France). HPLC grade formic acid (No. 7000027413) was obtained from Sigma Chemical Co. Ltd. (St. Louis, MO, USA).

2.2. Study protocol and sample collection

All protocols and the care of the rats were in accordance with the institutional guidelines for animal use in research. Male Sprague-Dawley rats (200 ± 20 g) were obtained from Beijing Weitonglihua Laboratory Animal Technology Co. Ltd. (Beijing, China). All of the rats were raised at a standard temperature ($23 \pm 2\,^{\circ}C$) and humidity ($60 \pm 5\%$) in a controlled room with a light/dark cycle of 12 h. The rats underwent an adaptation period of seven days, during which the rats were fed commercial feed and drank water *ad libitum*. Then, the rats were transferred to individual metabolic cages and allowed to acclimatize for three additional days. During this period, the rats' rectal temperatures were measured three times per day using a digital thermometer (Shanghai Huachen Medical Instruments Co. Ltd.) for monitoring the regular rhythm of body temperatures. The rats with temperature differences that were greater than $0.5\,^{\circ}C$ were excluded. Sixteen qualified rats were chosen and randomly divided into two groups, including the normal control group (CG) and the pyrexia model group (PG). The PG rats were subcutaneously injected with a 20% aqueous suspension of yeast (15 mL/kg) in the back of the rats. The CG rats were given an equal volume of 0.9% saline in parallel. The rectal temperature was measured, and the urine was collected at the time-points of 0, 5, 9, 13, 25, 37, 49, 61 and 73 h after administration. Each urine sample was centrifuged at 14,000 rpm for 10 min at $4\,^{\circ}C$, and the supernatant was collected and stored at $-20\,^{\circ}C$ until use.

2.3. Urine sample preparation and UPLC Q-TOF/MS analysis

Before the analysis, urine samples were thawed at room temperature, diluted at a ratio of 2:1 (v/v) using ultra high purity water, vortex mixed and centrifuged at 14,000 rpm for 10 min at $4\,^{\circ}C$. Then, the supernatants were subjected to the UPLC Q-TOF/MS system for analysis. The analysis was performed using a Waters Acquity^{TM} Ultra Performance LC system (Waters Corp., Milford, MA) connected to a Xevo^{TM} G2-Q-TOF mass spectrometer (Waters MS Technologies, Manchester, UK) that was equipped with an electrospray ionization (ESI) source, which was operated in the positive mode. The separation conditions and mass spectrometry parameters were described in our previous reports [11,17]. An MS^{E} technology was used for the data collection, and the parameters were set as follows: function 1, 6 eV collision energy; function 2, collision energy ramp of 20–40 eV.

2.4. Data analysis

The raw mass data were analyzed using the Applied Waters Markerlynx XS software (Waters Corporation, Milford, MA, USA), which could transform the raw data into a single matrix containing aligned peaks with t_r-m/z pairs, normalized peak intensities and sample names. For extracting data from the raw file and for detecting potential markers, the retention time range was set at 0–11.5 min; the mass range was set at 50–1000 amu; and the mass tolerance was set at 0.01. For detecting chromatographic peaks in the Apex Track Peak, the peak width at 5% height was set at 1.00, and the peak-to-peak baseline noise was set at 0.00. For collecting parameters, the marker intensity threshold was set at 1000 cps; the mass window was set at 0.02 amu; and the retention time window was 0.20 min. The noise elimination level was 6. This process provides an alignment of drifts (retention time and accurate mass) in data and ensures that a chromatographic peak is identified using identical parameters for each sample. Subsequently, a list of intensities or peak areas of the peaks was then generated for the first chromatogram, using the t_r-m/z pairs as identifiers. This procedure was applied for each UPLC/MS analysis. The ion intensities or peak area for each peak detected were also normalized within each

sample to the sum of the peak intensities in that sample. The three-dimensional data sets were introduced into the EZinfo 2.0 software (Waters Corporation, Milford, MA, USA) for PCA and OPLS-DA after missing values were assessed using the 80% rule [18].

For the identification of potential biomarkers, the following databases were used: HMDB (http://www.hmdb.ca/), KEGG (http://www.genome.jp/kegg/), Massbank (http://www.massbank.jp), Chemspider (http://www.chemspider.com), and METLIN (http://metlin.scripps.edu/).

Pearson correlation analysis was used to evaluate the relations of biomarkers and temperatures in rats using Microsoft Excel. Five biomarkers with high correlation factors to the temperatures were used for further ROC curve analysis using a web-based tool called ROCCET (ROC Curve Explorer & Tester, http://www.roccet.ca). The software was used with its default settings, except pareto scaling was used for data scaling. The statistical analysis of the rectal temperature was performed using the software SPSS 17.0 (SPSS Inc., Chicago, USA).

2.5. Network construction

A metabolic network was constructed using TCM grammar systems to illustrate the relations between five biomarkers and pyrexia. Prior knowledge regarding metabolic processes was obtained from a high-quality article concerning metabolic network reconstruction [19]. The biomarker-related proteins were derived from the STITCH database (http://stitch.embl.de/). To obtain more overall results, the parameter of the required confidence score was set higher than 0.1. Pyrexia-related small molecules, such as prostaglandin E_2 (PGE_2), cyclic adenosine monophosphate (cAMP), arginine vasopressin (AVP), nitric oxide (NO), arachidonate and prostaglandin $F_{2\alpha}$ ($PGF_{2\alpha}$), were collected from related studies [20–23]. To deduce the direct effects of biomarkers on pyrexia, the end node of the network was set using pyrexia-related small molecules. The network was visualized using the software Cytoscape.

3. Results and discussion

3.1. Yeast-induced pyrexia in rats

Fever is an obvious sign of infection and, thus, has been used in disease diagnosis for thousands of years. The measurement of the body temperature is the easiest clinical indicator in fever examination. To monitor the temperature development in the CG and PG rats, the rectal temperatures of the rats at different time points before and after yeast administration were recorded (Table 1). The temperature reached its peak 5 h after yeast injection, and then the temperature gradually decreased. At 37 h following yeast treatment, the temperature of the PG returned to the normal level compared with the CG. Using the independent samples *t*-test, statistically significant differences were observed for the temperatures of pyrexia rats at the 5 h, 9 h and 13 h time-points after modeling ($P < 0.001$, $P < 0.001$ and $P < 0.05$, respectively, *vs.* CG). With the development of fevers, the temperatures of the pyrexia rats remained higher than those temperatures of the control rats at the 25 h time-point; however, there was no statistical significance ($P > 0.05$). This result indicated that temperature could not act as the only indicator for the full reflection of biological processes that accompany fever, whereas the integrated effect of all of the metabolic disturbances, which are derived from fever or inflammation in yeast-deduced pyrexia rats, was related to temperature. Thus, finding those biomarkers related to rectal temperature was critical.

3.2. Multivariate data analysis

After the peak alignment, 4803 ion peaks were extracted using the software Markerlynx XS with the above-mentioned method. PCA is an unsupervised multivariate data analysis method that can give a comprehensive view of the clustering trend for multidimensional data [24]. This method was introduced to determine whether PG and CG could be separated. The PCA score plots of the PG and CG at different time-points are shown in Fig. 1. As exhibited in Fig. 1, the score plots of the 5 h, 9 h and 13 h time-points after yeast injection could be clearly separated using PCA. However, dots of the CG and PG mixed at the 25 h time-point, suggesting that the metabolic profiles of the PG and CG exhibited insignificant differences at 25 h after modeling. Not surprisingly, the result of the PCA was consistent with the temperature change track, indicating that the metabolite profile trend changed following the wake of the body temperature. Judging from the PCA maps, dots of the CG and PG showed a good separation at the 13 h time-point after the yeast injection, suggesting that the body remained at the pathological state, although the temperature was not significantly higher. At the 25 h time-point, although the temperature remaining higher than that of the normal body, the rats in the PG already reached the normal state, as determined from the PCA and the statistical results.

3.3. Detection of biomarker candidates

To characterize the potential biomarkers of the yeast-induced pyrexia model, the 5 h, 9 h and 13 h time-point data were chosen to perform a supervised multivariate data analysis using OPLS-DA. The VIP (variable importance in the projection) > 3 value was used to select the most representative biomarkers. Sixteen, fifteen and fifteen metabolites in the 5 h, 9 h and 13 h time-points, respectively, with higher contributions to the clustering analysis were selected as the potential biomarkers. These identified metabolites are summarized in Table 2. The verification method was based on previous reported methods [11,17]. The differences in the relative contents between the CG and the PG were marked, and the VIP values were noted.

3.4. Correlation analysis of potential biomarkers and rectal temperature

Pearson correlation analysis evaluated the relations of different potential biomarkers and rectal temperatures of in the pyrexia rats at the nine time-points (0 h, 5 h, 9 h, 13 h, 25 h, 37 h, 49 h, 61 h, and 73 h). Among the potential biomarkers of three time-points (5 h, 9 h and 13 h), indoleacrylic acid, 3-methyluridine and tryptophan at 5 h and nicotinuric acid and PI (37:3) at 9 h exhibited good correlation with the rectal temperature of the pyrexia rats, and their correlation coefficients were 0.898, 0.937, 0.913, 0.869 and 0.876, respectively (Fig. 2a–e). Simultaneously, the correlation coefficients between any two biomarkers were higher than 0.75 (Fig. 3a and supplementary material Table S1). Therefore, the variation in indoleacrylic acid, 3-methyluridine, tryptophan, nicotinuric acid and PI (37:3) extensively to the changes in the body temperature, and these metabolites should be further studied to explain the mechanism of inflammation-induced fever in rats. Of note, the metabolites that were found at 13 h did not show a good correlation with the temperature, although the results of the *t*-test and the PCA had a good differentiation, which might have arisen by the metabolites gradually returning to the normal state at the 13 h time-point. Therefore, the duration of 5–9 h after yeast injection was recommended to study the metabolite changes in yeast-induced pyrexia.

Supplementary material related to this article can be found, in the online version, at http://dx.doi.org/10.1016/j.jpba.2014.02.011.

Table 1
The results of rectal temperatures in the normal control group and the pyrexia model group.

Group	Rectal temperature (°C)								
	0 h	5 h	9 h	13 h	25 h	37 h	49 h	61 h	73 h
CG	34.1 ± 0.4	34.5 ± 0.4	34.6 ± 0.5	34.8 ± 0.5	34.6 ± 0.3	34.7 ± 0.4	34.3 ± 0.4	34.8 ± 0.4	33.9 ± 0.5
PG	33.9 ± 0.4	36.5 ± 0.3**	36.0 ± 0.2**	35.3 ± 0.3*	35.0 ± 0.4	34.7 ± 0.5	34.4 ± 0.2	34.8 ± 0.3	34.0 ± 0.4

Data were expressed as mean ± standard deviation.
* $P < 0.05$ compared with control by independent-sample t test.
** $P < 0.001$ compared with control by independent-sample t test.

3.5. Receiver operating characteristic curve analysis and prediction models

ROC curve analysis is widely considered the standard method to perform assessments [25]. Diagnostic accuracy is usually evaluated using the area under the ROC curve (AUC), which combines the sensitivity (true positive rate) and specificity (false positive rate) of a given biomarker for the diagnosis of a specific disease [26]. For the rectal temperature results, the 13 h time-point after modeling might be wrongly classed into the normal state because the temperature was not significantly higher than that of the normal body. Likewise, the 25 h time-point might be wrongly grouped into the pathological state. To evaluate the diagnostic capabilities of the five biomarkers that exhibited high correlation coefficients with the temperature, a two-stage ROC analysis was performed for each variable using the AUC, sensitivity and specificity assays. In the initial univariate ROC analysis, the ambiguous time-points of 13 h and 25 h were removed. All five biomarkers showed good diagnostic accuracy, with the AUC reaching 0.864–0.965 with high sensitivity and high specificity (Fig. 2f–j). In the second univariate ROC analysis, the 13 h and 25 h time-points were included and marked as the pathological state and normal state, respectively. After introducing the 13 h and 25 h time-points, the AUC reached 0.843–0.933 (Fig. 2k–o). Therefore, the inclusion of the 13 h and 25 h time-points slightly affected the prediction ability of the diagnostic results, which showed a better diagnostic accuracy for fever than for the body temperature.

ROC curve-based model evaluation was also performed to assess the integrated predictive power of the combined five biomarkers for distinguishing pyrexia and the normal state. The AUC values

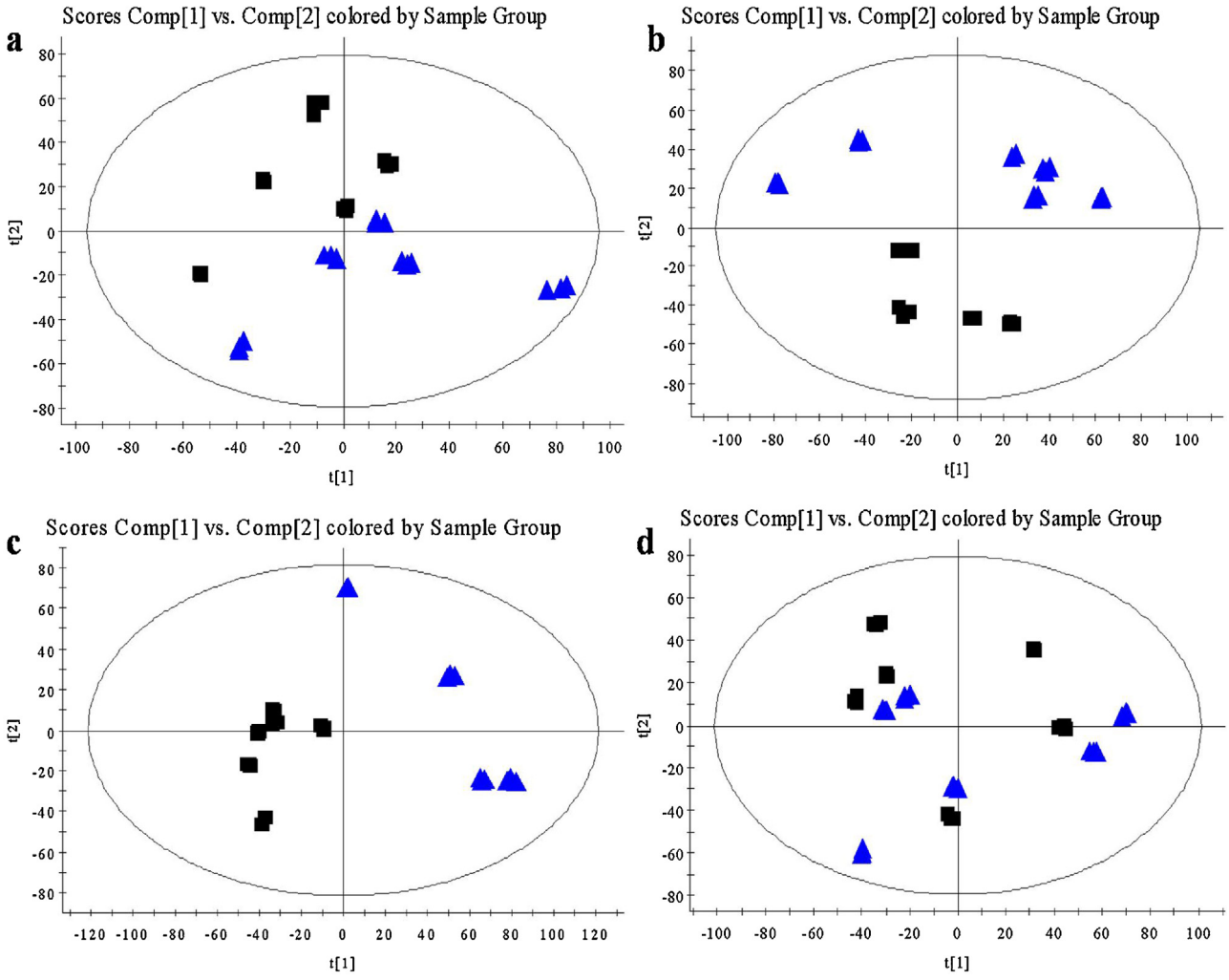

Fig. 1. Score plots of the CG (■) and PG (▲) from PCA models at different time-points. (a) 5 h. (b) 9 h. (c) 13 h. (d) 25 h.

Table 2
Most prominent metabolites discriminated of yeast-induced pyrexia rats at the time-points of 5 h, 9 h and 13 h.

Time	No.	t_r-m/z	VIP	Metabolites	Levels in pyrexia
5 h	1	0.6847–212.1034	10.43	3-Methoxytyrosine	↓*
	2	0.5221–104.1074	8.32	Gamma-aminobutyric acid	↑***
	3	**3.3211–188.0709**	**8.29**	**Indoleacrylic acid**	↑***
	4	0.6072–116.0710	6.84	Proline	↑**
	5	**0.6898–259.0929**	**6.35**	**3-Methyluridine**	↑*
	6	3.4248–206.0453	6.21	Xanthurenic acid	↓*
	7	3.6454–160.0971	6.20	Methylbutyrylglycine	↓**
	8	2.8333–252.0730	5.62	Deoxyadenosine	↑***
	9	**3.3200–205.0966**	**5.00**	**Tryptophan**	↑***
	10	0.6783–127.0488	4.87	Imidazoleacetate	↑***
	11	0.6373–144.1008	4.39	Proline betaine	↓***
	12	3.7831–190.0503	4.26	Kynurenic acid	↑*
	13	6.6141–335.0221	3.59	Nicotinamide ribotide	↓***
	14	1.9301–174.1239	3.57	N-Acetylleucine	↓*
	15	11.0093–913.5141	3.53	PI (22:5/18:0)[a]	↑***
	16	11.3634–812.4416	5.45	PE (22:6/20:4)[b]	↑***
9 h	1	0.5611–114.0666	8.86	Creatinine	↑**
	2	0.6725–212.1032	8.53	3-Methoxytyrosine	↓**
	3	0.6587–176.1016	8.19	Citrulline	↑***
	4	4.8598–194.0814	7.80	Phenylacetylycine	↓***
	5	**3.6247–181.0608**	**6.76**	**Nicotinuric acid**	↑***
	6	0.5293–118.0614	6.57	Glycocyamine	↑***
	7	10.8402–274.2740	5.68	Hexadecasphinganine	↑*
	8	0.7009–150.0776	5.67	Methyladenine	↑***
	9	5.0161–162.0552	5.57	Indole-3-carboxylic acid	↑***
	10	0.6257–189.1234	5.48	N-Acetyllysine	↓***
	11	0.7429–146.0928	5.31	4-Guanidinobutanoic acid	↓**
	12	0.6677–127.0480	5.23	Imidazoleacetate	↓***
	13	10.8631–318.3000	4.78	Phytosphingosine	↑*
	14	0.6343–144.1016	4.33	Proline betaine	↑*
	15	**11.2093–913.5191**	**3.13**	**PI (37:3)[a]**	↑*
13 h	1	10.8302–274.2741	10.23	Hexadecasphinganine	↑***
	2	10.8584–318.3002	9.17	Phytosphingosine	↑*
	3	0.5629–118.0868	7.72	5-Aminopentanoic acid	↑***
	4	2.7822–220.1184	7.31	Pantothenic acid	↓***
	5	0.6107–143.0820	7.05	Unknown	↓***
	6	0.6006–116.0712	5.59	Proline	↑***
	7	0.6514–176.1017	5.35	Citrulline	↑***
	8	4.8570–194.0816	5.03	Phenylacetylycine	↓***
	9	0.6226–189.1236	4.86	N-Acetyllysine	↓***
	10	3.7885–190.0504	4.74	Kynurenic acid	↓***
	11	0.5262–148.0605	4.58	N-Methyl-D-aspartic acid	↑***
	12	0.7338–136.0623	4.15	Adenine	↑**
	13	0.5656–114.0668	4.06	Creatinine	↑*
	14	0.5230–104.1074	3.87	Gamma-aminobutyric acid	↑*
	15	0.7443–146.0929	3.77	4-Guanidinobutanoic	↓**

The metabolites marked with bold represented the high correlations between the relative intensity and the body temperature.
↑: Compared with the control group using the peak areas, the compound was up-regulated in the model group.
↓: Compared with the control group using the peak areas, the compound was down-regulated in the model group.
[a] PI represents phosphatidylinositol.
[b] PE represents phosphatidylethanolamine.
* $P<0.05$.
** $P<0.01$.
*** $P<0.001$.

that excluded and included the 13 h and 25 h time-points were 0.985 and 0.968, respectively (Fig. 3b and c). The results showed a good discriminating power between pyrexia and the normal state. The five biomarkers demonstrated satisfactory performance in the diagnosis of pyrexia.

3.6. Mechanism networks of biomarkers to pyrexia

Network models, which can provide an integrated view of biological processes at the molecular level, are useful tools for understanding how molecules and the interactions between the molecules determine cell functions [27]. In this paper, to illustrate the rationality of the five biomarkers related to pyrexia, a metabolic network was constructed using TCM grammar systems to describe the biomarker interactions with pyrexia-related molecules.

Fig. 4 shows the direct metabolic interactions of biomarkers with pyrexia-related small molecules. Four of five biomarkers could be found in pyrexia-related pathways, including indoleacrylic acid, 3-methyluridine, nicotinuric acid, and PI, which represents a class of molecules, with 13 in the network, including N-acetylglucosaminylphosphatidylinositol (GNA-PI), glucosaminylphosphatidylinositol (GlcN-PI), acylglucosaminylphosphatidylinositol (GlcN-acyl-PI), ethanolaminephosphate-2-mannosealpha1-4glucosaminyl-acyl-phosphatidylinositol ((EtNP-2)Man(alpha1-4)GlcN-acyl(alpha1-6)PI), 1-phosphatidyl-1-D-myo-inositol 4-phosphate, 1-phosphatidyl-D-myo-inositol 4,5-bisphosphate, D-glucosaminylphosphatidylinositol, D-glucosaminylphosphatidylinositol, (ethanolaminephosphate) mannose-mannose-(ethanolaminephosphate)mannose- glucosaminyl-acyl-phosphatidylinositol (EtNP-Man-Man-(EtNP)

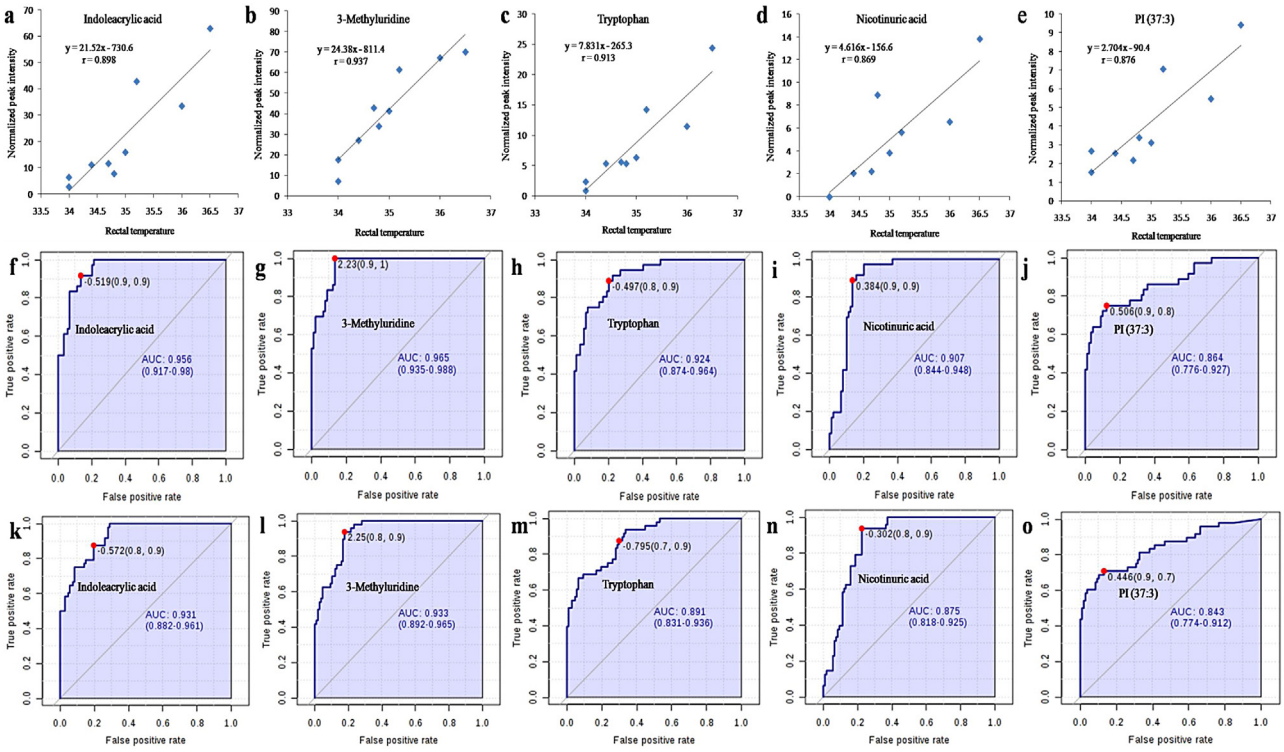

Fig. 2. Results of the correlation analysis and ROC curve evaluations. (a)–(e) Correlation analysis plots between biomarkers and rectal temperatures. (f)–(j) Diagnostic efficacy evaluation using ROC curves exclude the 13 h and 25 h time-points. (k)–(o) Diagnostic efficacy evaluation using ROC curves include the 13 h and 25 h time-points. The optimal cutoffs using the closest to top-left corner and the area under ROC curves with a 95% confidence interval were displayed.

Man-GlcN-acyl-PI), alpha-mannose-glucosaminyl-acyl-phosphatidylinositol (Man(alpha1-4)GlcN-acyl(alpha1-6)PI), mannose-alpha1-6(ethanolaminephosphate-2) mannosealpha1-4(acyl) glucosaminyl-phosphatidylinositol (Man-(EtNP)Man-GlcN-acyl-PI), mannosealpha1-2mannosealpha1-6(ethanolamine-phosphate-2)mannosealpha1-4glucosaminyl-acyl-phosphatidylinositol (Man-Man-(EtNP)Man-GlcN-acyl-PI), N-acetyl-D-glucosaminylphosphatidylinositol and phosphatidylinositol-3,4,5-trisphosphate. These 13 small molecules, which belong to PI, participate in prostaglandin E_2, nitric oxide, and arachidonate production, as shown in Fig. 4, which could ultimately influence the pyrexia process.

As shown in Fig. 4a, 3-methyluridine, which is one of the other four biomarkers, plays an important role in activating Enzyme 5.4.99.2, followed by a series of reactions. Enzyme 5.4.99.2 promotes the production of succinyl-CoA, which leads to the accumulation of CoA and prepares raw materials for arachidonate production. Arachidonate is associated with a variety of inflammation-related metabolic pathways. By the cyclooxygenase pathway, arachidonate generates PGE_2, which can pass through the blood-brain barrier, permeate into hypothalamus regions and, finally, induce pyrexia [28].

As shown in Fig. 4b, nicotinuric acid, which is another biomarker, contributes to induce Enzyme 5.3.99.2, which can catalyze the production process of prostaglandin H_2 and prostaglandin D_2, which are the raw materials for PGE_2 and PGF_2 synthesis, respectively [29]. Then, PGE_2, the main mediator of fevers, diffuses across the blood brain barrier, binds to specific PGE_2 receptors in the preoptic

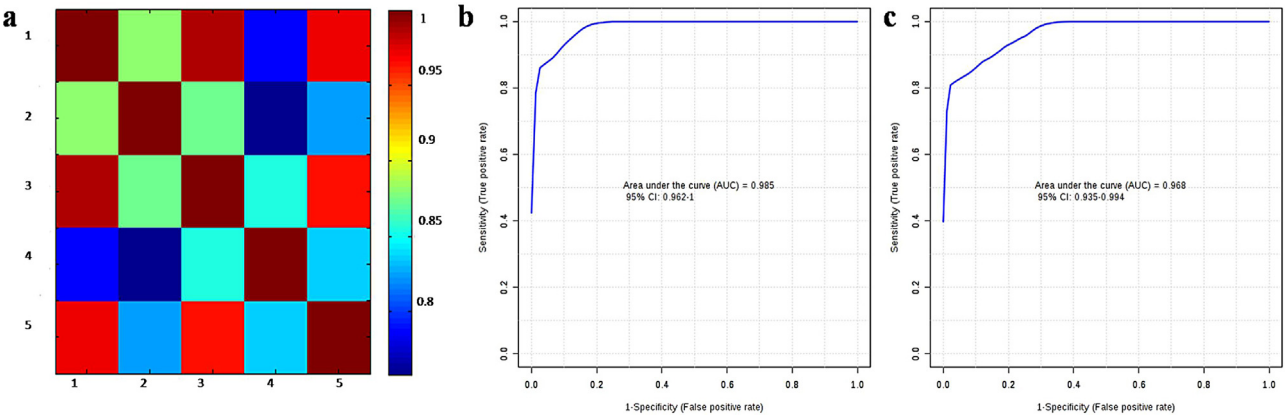

Fig. 3. Results of Pearson correlation analysis and ROC curve-based model evaluation. (a) Pearson correlation analysis of the five biomarkers. 1–5 represent indoleacrylic acid, 3-methyluridine, tryptophan, nicotinuric acid and PI (37:3). (b) ROC curve-based model evaluation to diagnose the predictive power of the five biomarkers. The 13 h and 25 h time-points were excluded. (c) ROC curve-based model evaluation to diagnose the predictive power of the five biomarkers. The 13 h and 25 h time-points were included.

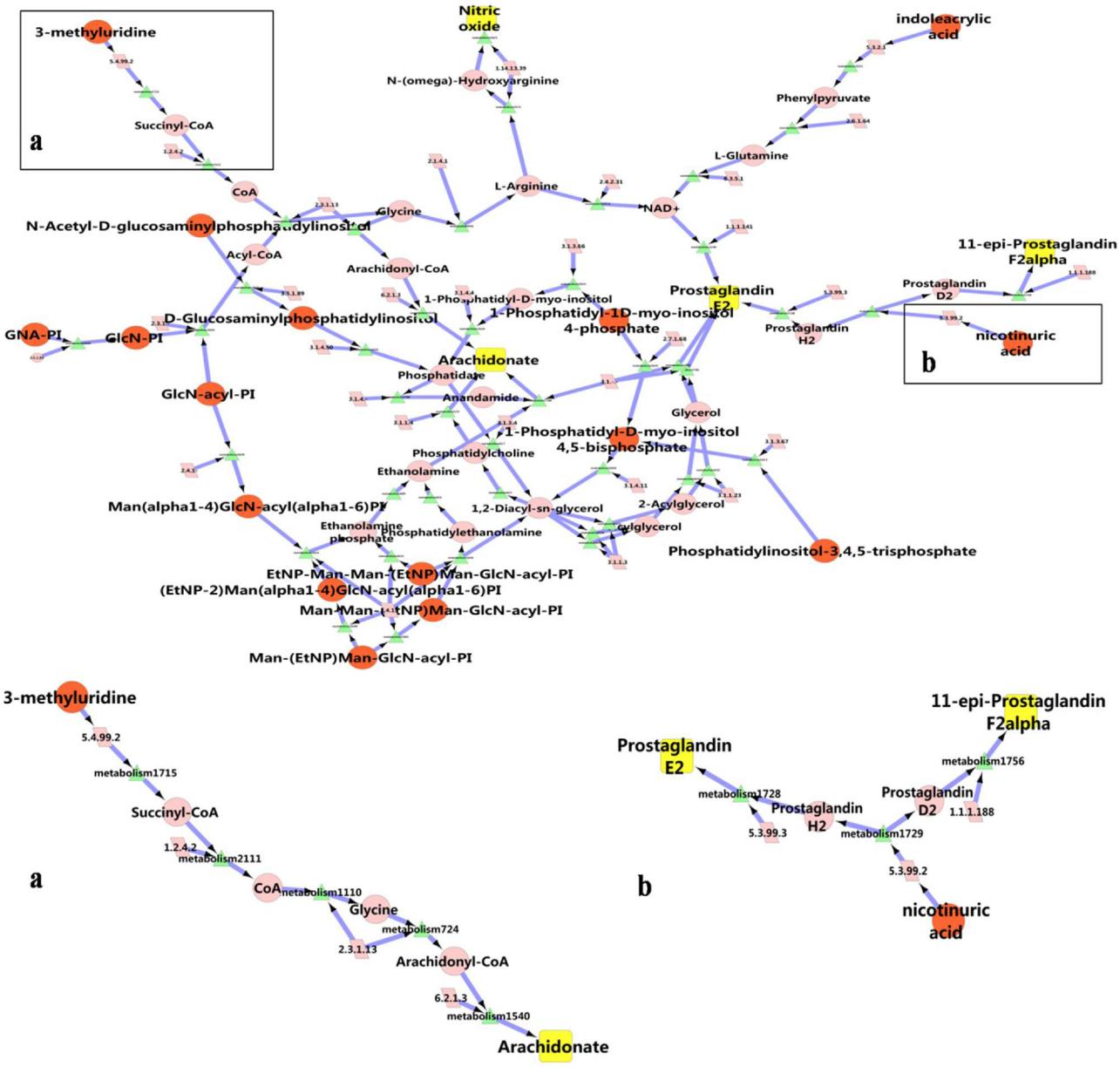

Fig. 4. Mechanism networks of biomarkers of pyrexia. Biomarkers are shown as orange circles. The fever-related small molecules are yellow squares. Green triangles denote metabolic reactions, and pink parallelograms denote enzymes. Edges with arrows represent the directions of reactions. Pink circles denote reaction intermediates that participate in the linkage of biomarkers to pyrexia. (For interpretation of the references to color in this figure legend, the reader is referred to the web version of the article.)

area and then activates thermal neurons in the anterior hypothalamus to a higher thermal balance point.

In our previous study, four metabolites participating in the tryptophan metabolic pathway, including tryptophan, kynurenic acid, xanthurenic acid and nicotinamide ribotide, were found to be disturbed in yeast-induced fever rats [11], indicating that tryptophan metabolism might contribute to fever. It had been reported that the activation of 5-hydroxytryptamine$_{1A}$ receptors, which play an important role in tryptophan metabolism, causes a robust fall in body temperature [30]. Some studies also found that the injection of IL-1β stimulates tryptophan hydroxylase expression in the hypothalamus and further discovered the synthesis or release of serotonin in the rat hypothalamus [31]. Because the relation between tryptophan metabolism and fever remained a hypothesis, we were not able to include tryptophan in the network models. However, this hypothesis was supported by our present and previous findings.

4. Conclusions

In the current study, a dynamic and continuous metabolic footprint analysis technique, which coincided with the metabolite changing process of organisms, was initially developed to reveal the changing track pathways of organisms and to clarify the mechanisms of the febrile response. Then, good clustering features between the normal control group and the pyrexia model group were found at the 5 h, 9 h and 13 h time-points following treatment with PCA and OPLS-DA, and the potential biomarkers were determined by combining several available databases. Next, Pearson correlation analysis was used to assess the relations among the fluctuations in potential biomarkers, including indoleacrylic acid, 3-methyluridine, tryptophan, nicotinuric acid and PI (37:3), the pharmacological index, namely, the changing trend of temperature. Last, ROC curves were achieved, and the metabolic network constructed by TCM grammar systems was introduced to validate

the rationality of the five biomarkers. This paper proposed a useful strategy for selecting rational biomarkers from many potential biomarkers derived from a metabolomic study of fever, thus providing a meaningful choice for evaluating biomarkers of other acute metabolic diseases.

Three steps occur during the analysis of a potential biomarker to a true biomarker: discovery, evaluation, and development. During the evaluation stage, to exclude false positive biomarkers due to a lack of analytical precision or rigor in data processing steps, the variability within a period in the control group should be evaluated. Considering the current study, to obtain more reliable biomarkers, future studies will focus on investigating the content variability of the five biomarkers screened by the above-mentioned strategy.

Acknowledgments

This study was supported in part by the National Natural Science Foundation of China (81173649/H2817) and by the Foundation of Independent Topics at Beijing University of Chinese Medicine (0100601055).

References

[1] C.A. Dinarello, Interleukin-1 and the pathogenesis of the acute-phase response, N. Engl. J. Med. 311 (1984) 1413–1418.
[2] B.G. Southorn, J.R. Thompson, Time course changes in blood metabolites during endotoxin fever in sheep, Can. J. Vet. Res. 50 (1986) 374–379.
[3] C.M. Blatteis, The onset of fever: new insights into its mechanism, Prog. Brain Res. 162 (2007) 3–14.
[4] M.D. Dogan, H. Ataoglu, E.S. Akarsu, Effects of different serotypes of *Escherichia coli* lipopolysaccharides on body temperature in rats, Life Sci. 67 (2000) 2319–2329.
[5] S. Liu, F. Lu, X. Wang, W. Sun, P. Chen, W. Dong, Metabolomic study of a rat fever model induced with 2,4-dinitrophenol and the therapeutic effects of a crude drug derived from *Coptis chinensis*, Am. J. Chin. Med. 39 (2011) 95–109.
[6] J. Tomazetti, D.S. Avila, A.P. Ferreira, J.S. Martins, F.R. Souza, C. Royer, M.A. Rubin, M.R. Oliveira, H.G. Bonacorso, M.A. Martins, N. Zanatta, C.F. Mello, Baker yeast-induced fever in young rats: characterization and validation of an animal model for antipyretics screening, J. Neurosci. Methods 147 (2005) 29–35.
[7] P. Antonisamy, V. Duraipandiyan, S. Ignacimuthu, Anti-inflammatory, analgesic and antipyretic effects of friedelin isolated from *Azima tetracantha* Lam. in mouse and rat models, J. Pharm. Pharmacol. 63 (2011) 1070–1077.
[8] J.J. Loux, P.D. DePalma, S.L. Yankell, Antipyretic testing of aspirin in rats, Toxicol. Appl. Pharmacol. 22 (1972) 672–675.
[9] S. Sasmal, S. Majumdar, M. Gupta, A. Mukherjee, P. Mukherjee, Pharmacognostical, phytochemical and pharmacological evaluation for the antipyretic effect of the seeds of Saraca asoca Roxb, Asian Pac. J. Trop. Biomed. 2 (2012) 782–786.
[10] A.I. Braude, C.J. Mc, H. Douglas, Fever from pathogenic fungi, J. Clin. Invest. 39 (1960) 1266–1276.
[11] X. Gao, M. Guo, B. Zhao, L. Peng, J. Su, X. Bai, J. Li, Y. Qiao, A urinary metabonomics study on biochemical changes in yeast-induced pyrexia rats: a new approach to elucidating the biochemical basis of the febrile response, Chem. Biol. Interact. 204 (2013) 39–48.
[12] N.J. Waters, E. Holmes, A. Williams, C.J. Waterfield, R.D. Farrant, J.K. Nicholson, NMR and pattern recognition studies on the time-related metabolic effects of alpha-naphthylisothiocyanate on liver, urine, and plasma in the rat: an integrative metabonomic approach, Chem. Res. Toxicol. 14 (2001) 1401–1412.
[13] M. Mamas, W.B. Dunn, L. Neyses, R. Goodacre, The role of metabolites and metabolomics in clinically applicable biomarkers of disease, Arch. Toxicol. 85 (2011) 5–17.
[14] A. Koulman, G.A. Lane, S.J. Harrison, D.A. Volmer, From differentiating metabolites to biomarkers, Anal. Bioanal. Chem. 394 (2009) 663–670.
[15] N.A. Obuchowski, M.L. Lieber, F.H. Wians Jr., ROC curves in clinical chemistry: uses, misuses, and possible solutions, Clin. Chem. 50 (2004) 1118–1125.
[16] J. Yan, Y. Wang, S.J. Luo, Y.J. Qiao, TCM grammar systems: an approach to aid the interpretation of the molecular interactions in Chinese herbal medicine, J. Ethnopharmacol. 137 (2011) 77–84.
[17] X. Gao, M. Guo, L. Peng, B. Zhao, J. Su, H. Liu, L. Zhang, X. Bai, Y. Qiao, UPLC Q-TOF/MS-based metabolic profiling of urine reveals the novel antipyretic mechanisms of Qingkailing injection in a rat model of yeast-induced pyrexia, Evid.-Based Compl. Alt. Med. Vol. (2013), http://dx.doi.org/10.1155/2013/864747.
[18] S. Bijlsma, I. Bobeldijk, E.R. Verheij, R. Ramaker, S. Kochhar, I.A. Macdonald, B. van Ommen, A.K. Smilde, Large-scale human metabolomics studies: a strategy for data (pre-)processing and validation, Anal. Chem. 78 (2006) 567–574.
[19] H. Ma, A. Sorokin, A. Mazein, A. Selkov, E. Selkov, O. Demin, I. Goryanin, The Edinburgh human metabolic network reconstruction and its functional analysis, Mol. Syst. Biol. 3 (2007) 135.
[20] W.W. Blessing, 5-Hydroxytryptamine 1A receptor activation reduces cutaneous vasoconstriction and fever associated with the acute inflammatory response in rabbits, Neuroscience 123 (2004) 1–4.
[21] C.C. Chio, S.M. Tsai, J.J. Wang, M.T. Lin, 5-HT2A-mu opioid receptor mechanisms in the hypothalamus mediate interleukin-1beta fever in rats, Neurosci. Lett. 381 (2005) 6–11.
[22] R.C. Reis, H.O. Brito, D. Fraga, D.A. Cabrini, A.R. Zampronio, Central substance P NK(1) receptors are involved in fever induced by LPS but not by IL-1beta and CCL3/MIP-1alpha in rats, Brain Res. 1384 (2011) 161–169.
[23] D.M. Soares, F. Hiratsuka Veiga-Souza, A.S. Fabricio, F. Javier Minano, G.E. Petto Souza, CCL3/macrophage inflammatory protein-1alpha induces fever and increases prostaglandin E2 in cerebrospinal fluid of rats: effect of antipyretic drugs, Brain Res. 1109 (2006) 83–92.
[24] W. Weckwerth, K. Morgenthal, Metabolomics: from pattern recognition to biological interpretation, Drug Discov. Today 10 (2005) 1551–1558.
[25] J. Xia, D.I. Broadhurst, M. Wilson, D.S. Wishart, Translational biomarker discovery in clinical metabolomics: an introductory tutorial, Metabolomics 9 (2013) 280–299.
[26] T. Poynard, P. Halfon, L. Castera, M. Munteanu, F. Imbert-Bismut, V. Ratziu, Y. Benhamou, M. Bourliere, V. de Ledinghen, G. FibroPaca, Standardization of ROC curve areas for diagnostic evaluation of liver fibrosis markers based on prevalences of fibrosis stages, Clin. Chem. 53 (2007) 1615–1622.
[27] A.L. Barabasi, Z.N. Oltvai, Network biology: understanding the cell's functional organization, Nat. Rev. Genet. 5 (2004) 101–113.
[28] S. Gu, N. Yin, J. Pei, L. Lai, Understanding traditional Chinese medicine anti-inflammatory herbal formulae by simulating their regulatory functions in the human arachidonic acid metabolic network, Mol. Biosyst. 9 (2013) 1931–1938.
[29] S. Malhotra, S.S. Deshmukh, S.G. Dastidar, COX inhibitors for airway inflammation, Expert. Opin. Ther. Targets 16 (2012) 195–207.
[30] J.F. Cryan, P. Kelliher, J.P. Kelly, B.E. Leonard, Comparative effects of serotonergic agonists with varying efficacy at the 5-HT(1A) receptor on core body temperature: modification by the selective 5-HT(1A) receptor antagonist WAY 100635, J. Psychopharmacol. 13 (1999) 278–283.
[31] F.S. Chueh, C.P. Chang, C.C. Chio, M.T. Lin, Puerarin acts through brain serotonergic mechanisms to induce thermal effects, J. Pharmacol. Sci. 96 (2004) 420–427.